Optimization of Low-profile WAIM Superstrates over Patch Arrays

G. Oliveri, A. Polo, M. Salucci, G. Gottardi, and A. Massa

Contents

1 Multi-frequency WAIM Analysis

In this section we will extend our analysis to the *multifrequency* case. We will optimize the WAIM layers in order to have an improvement in the performance not only at the working frequency f_0, but also in a user-defined band of frequencies.

For this test case we will use a new substrate $(FR-4)$, having $\varepsilon^{sub} = 4.3$, $tan\delta = 0.025$ and the analysis will be performed on 3 frequency samples: $0.9f_0$, f_0 and $1.1f_0$.

1.1 Test Case #1 - Multi-frequency - 2 Isotropic WAIM Layers - $\varepsilon^1 = \varepsilon^2 = [1 : 35] + j0$ - Square Lattice - $\varepsilon^{sub} = 4.3 + j0.1075$ Tests

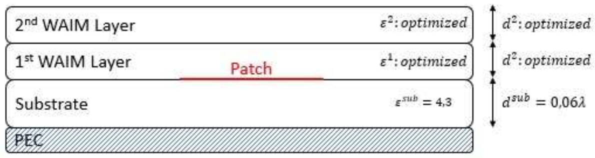

Figure 1: Test Case Schema.

Simulation Parameters:

- Frequency: $f_0 = 10[GHz]$;
- Frequency min: $f_{min} = 0.9f_0$;
- Frequency max: $f_{max} = 1.1f_0$;
- Frequency samples: $F = 3$;
- Patch dimensions: $w = 0.307$, $l = 0.2125$ $[\lambda]$;
- Probe position: $x = 0.0705$, $y = 0.1535$ $[\lambda]$;
- Substrate: $\varepsilon_x = 4.3 + j0.1075$, $\varepsilon_y = 4.3 + j0.1075$, $\varepsilon_z = 4.3 + j0.1075$, $d = 0.06[\lambda]$
- Floquet coefficient $= 121$;
- Lattice basis: $s_1 = (0.5, 0.0)$, $s_2 = (0.0, 0.5)$ $[\lambda]$;

Analysis Parameters:

- Samples analysis (phi cuts): $\theta \in [0, 90]$ $[deg]$, $\varphi \in [0, 90]$ $[deg]$, $\theta_{samples} = 91$, $\varphi_{samples} = 3$;
- Samples analysis (3D plots): $\theta \in [-90, 90]$ $[deg]$, $\varphi \in [-90, 90]$ $[deg]$, $\theta_{samples} = 36$, $\varphi_{samples} = 21$;

PSO Synthesis Parameters:

- Number of WAIM Layers: $N = 2$;
- Unknowns: $U = 4$;
- Unknown ranges: $\varepsilon = [1 : 35] + j0$, $d = [0.033 : 0.5]$ $[\lambda]$;
- Swarm size: $P = 12$;
- Max iteration number: $I = 200$;
- Inertial weight= 0.4;
- Alpha= 0.4;
- Beta= 0.4;
- C1= 2.0;
- C2= 2.0;
- Random seeds= 6, 12, 26, 33, 46, 51, 65, 77, 98;
- No-WAIM case implemented by the first particle at the 1^{st} iteration;
- Samples synthesis (phi cuts): $\theta \in [0, 90]$ $[deg]$, $\varphi \in [0, 90]$ $[deg]$, $\theta_{samples} = 7$, $\varphi_{samples} = 3$;

Optimization Results

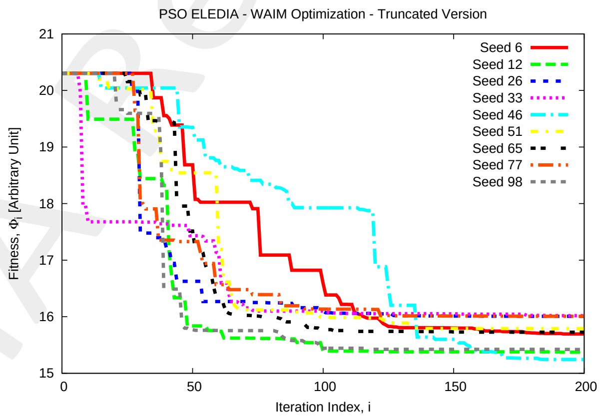

Figure 2: Fitness Dynamics.

$$Best\,result:\ Seed\,46$$

$$Simulation\,time\,(Truncated):\ 1223m\,37s$$

Tool	*Optimal Solution*				*Fitness Value*	
	$\varepsilon_x^1 = \varepsilon_y^1 = \varepsilon_z^1$	$h^1\ [\lambda]$	$\varepsilon_x^2 = \varepsilon_y^2 = \varepsilon_z^2$	$h^2\ [\lambda]$	$\Phi_{i=0}$	$\Phi_{I=200}$
Truncated	1.002	0.083	3.051	0.496	20.303	15.244

Table 1: *Seed* 46 Optimal Solution.

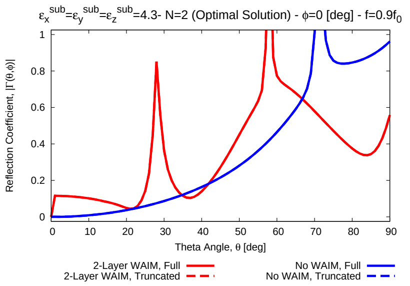

(*a*) Γ, $\varphi = 0[deg]$, $f = 0.9f_0$

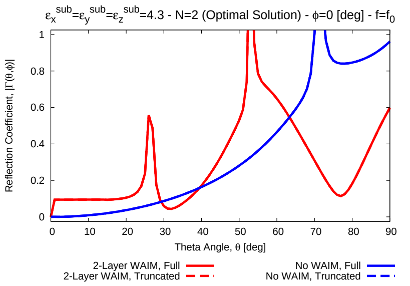

(*b*) Γ, $\varphi = 0[deg]$, $f = f_0$

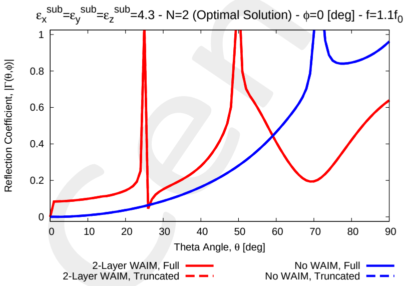

(*c*) Γ, $\varphi = 0[deg]$, $f = 1.1f_0$

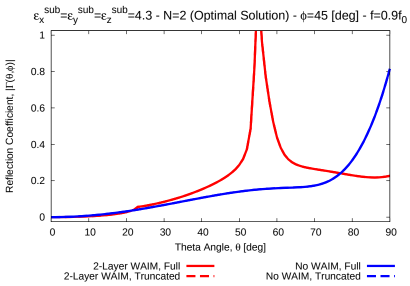

(*d*) Γ, $\varphi = 45[deg]$, $f = 0.9f_0$

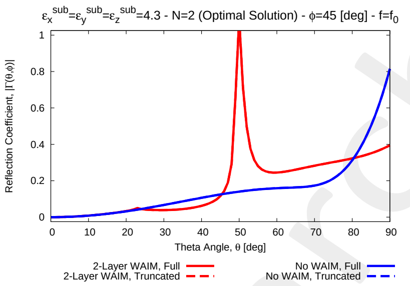

(*e*) Γ, $\varphi = 45[deg]$, $f = f_0$

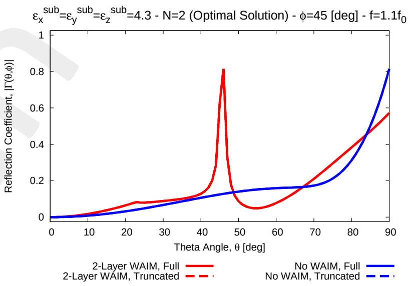

(*f*) Γ, $\varphi = 45[deg]$, $f = 1.1f_0$

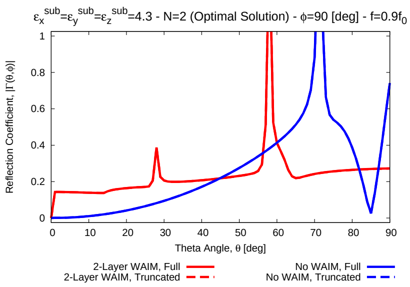

(*g*) Γ, $\varphi = 90[deg]$, $f = 0.9f_0$

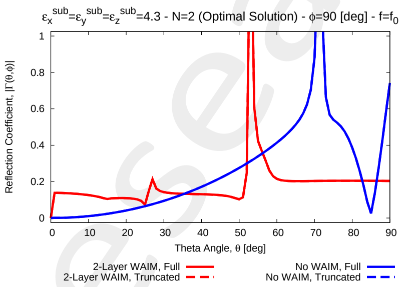

(*h*) Γ, $\varphi = 90[deg]$, $f = f_0$

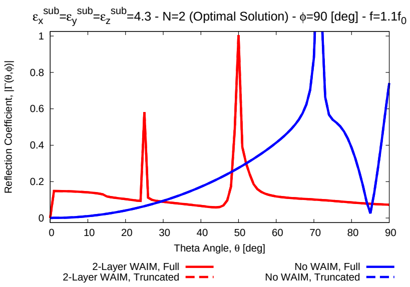

(*i*) Γ, $\varphi = 90[deg]$, $f = 1.1f_0$

Figure 3: *Seed* 46, Reflection Coefficient along φ cuts, 2 Layers WAIM.

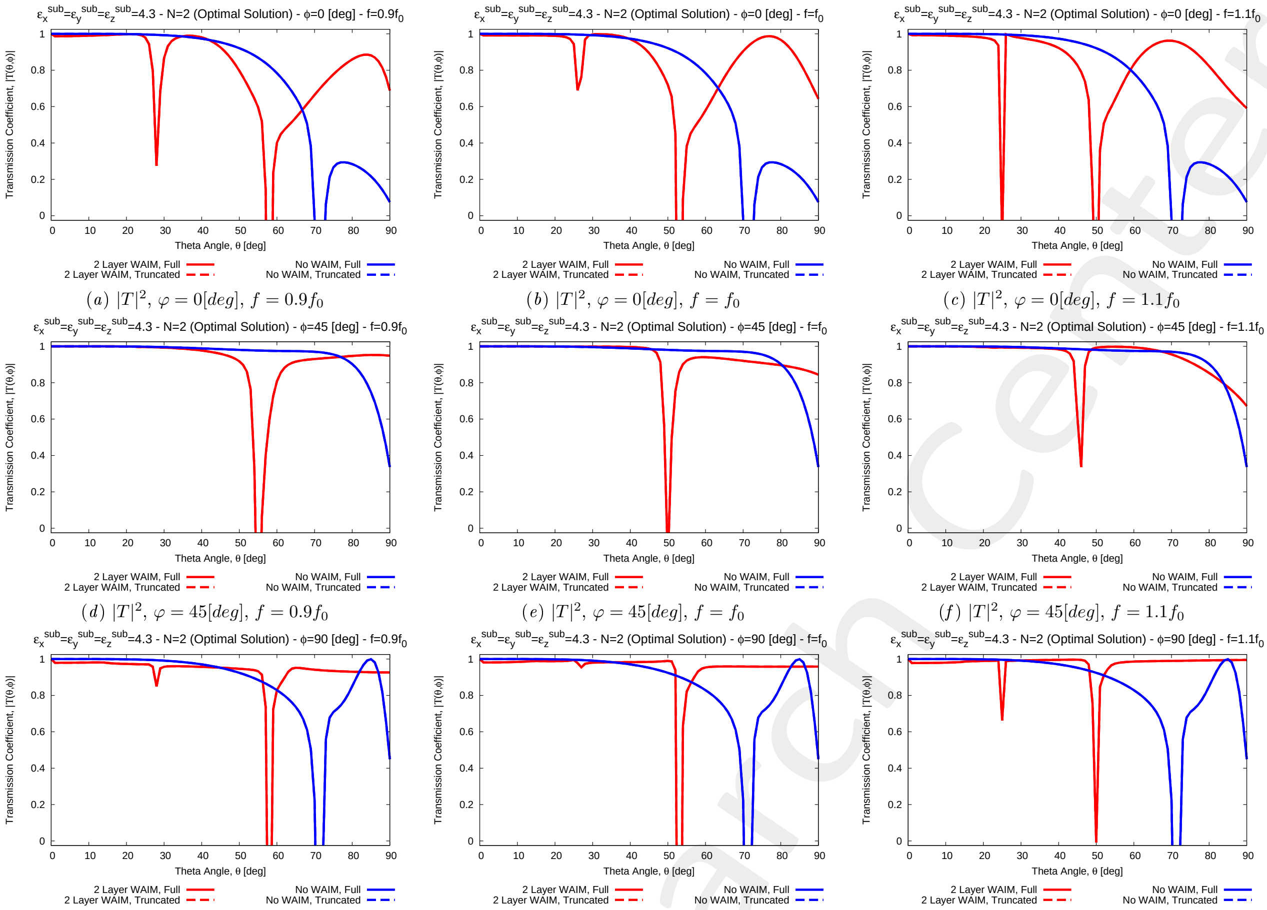

(a) $|T|^2$, $\varphi = 0[deg]$, $f = 0.9f_0$ (b) $|T|^2$, $\varphi = 0[deg]$, $f = f_0$ (c) $|T|^2$, $\varphi = 0[deg]$, $f = 1.1f_0$

(d) $|T|^2$, $\varphi = 45[deg]$, $f = 0.9f_0$ (e) $|T|^2$, $\varphi = 45[deg]$, $f = f_0$ (f) $|T|^2$, $\varphi = 45[deg]$, $f = 1.1f_0$

(g) $|T|^2$, $\varphi = 90[deg]$, $f = 0.9f_0$ (h) $|T|^2$, $\varphi = 90[deg]$, $f = f_0$ (i) $|T|^2$, $\varphi = 90[deg]$, $f = 1.1f_0$

Figure 4: $Seed\,46$, Transmission Coefficient along φ cuts, 2 Layers WAIM.

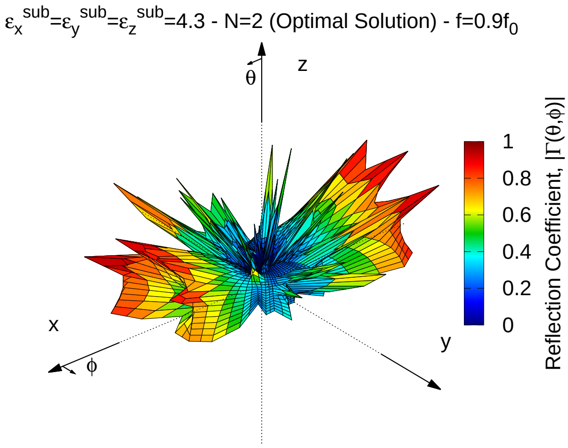

(a) Γ, 2 Layers WAIM, $f = 0.9 f_0$

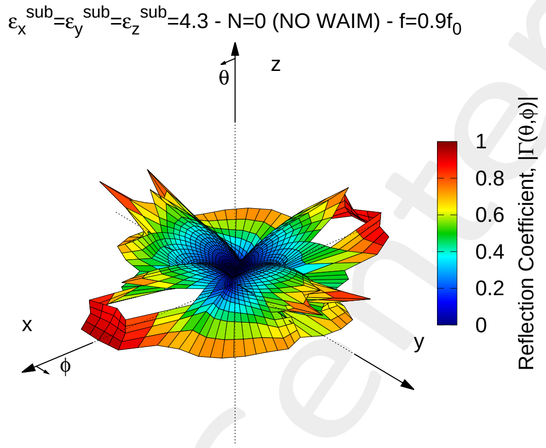

(b) Γ, No-WAIM, $f = 0.9 f_0$

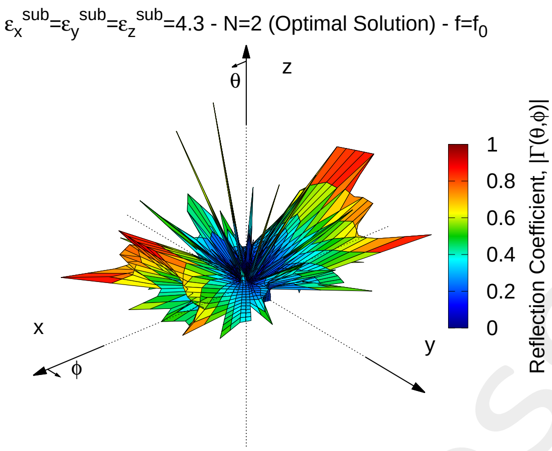

(c) Γ, 2 Layers WAIM, $f = f_0$

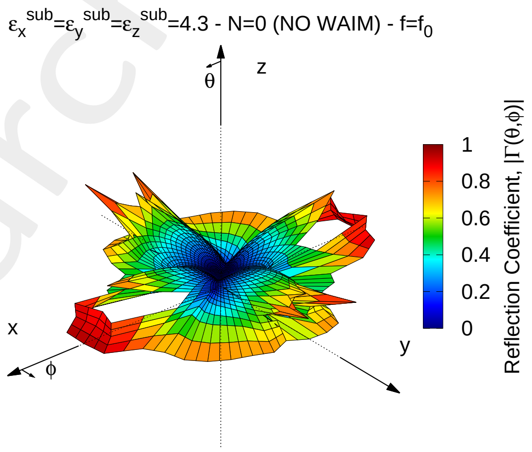

(d) Γ, No-WAIM, $f = f_0$

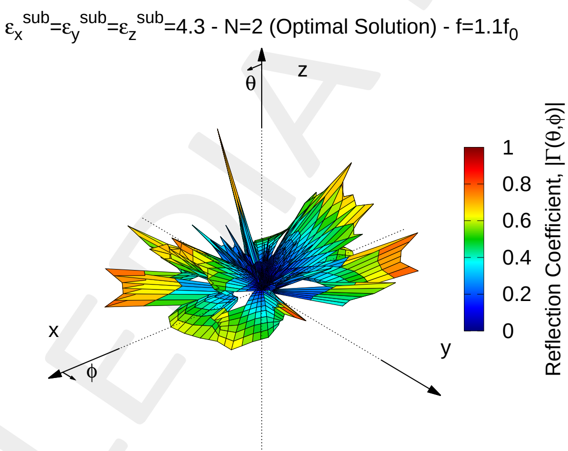

(e) Γ, 2 Layers WAIM, $f = 1.1 f_0$

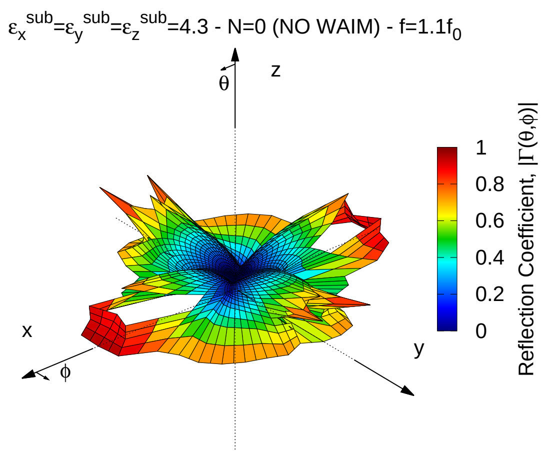

(f) Γ, No-WAIM, $f = 1.1 f_0$

Figure 5: *Seed* 46, 3D Reflection Coefficient.

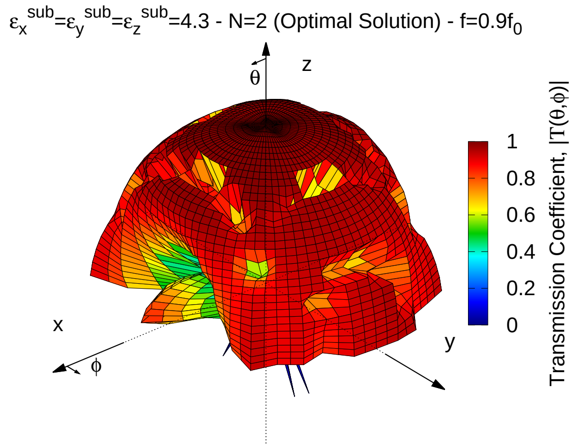

(a) $|T|^2$, 2 Layers WAIM, $f = 0.9f_0$

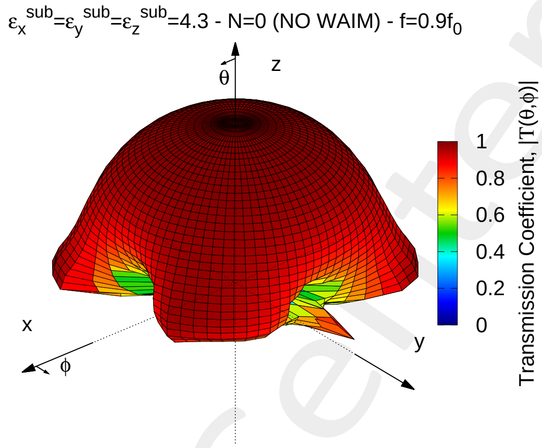

(b) $|T|^2$, No-WAIM, $f = 0.9f_0$

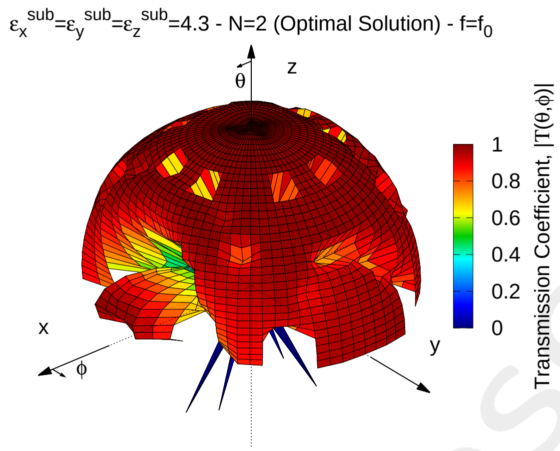

(c) $|T|^2$, 2 Layers WAIM, $f = f_0$

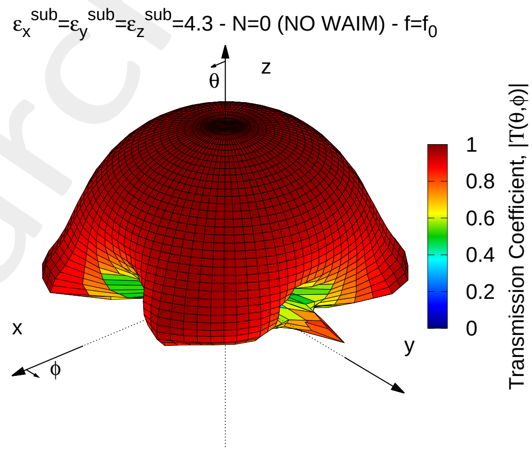

(d) $|T|^2$, No-WAIM, $f = f_0$

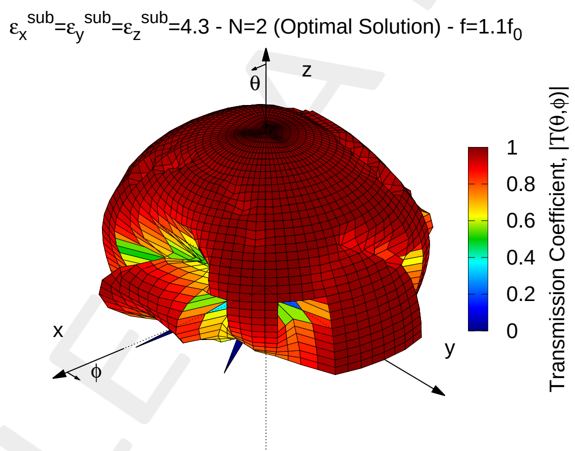

(e) $|T|^2$, 2 Layers WAIM, $f = 1.1f_0$

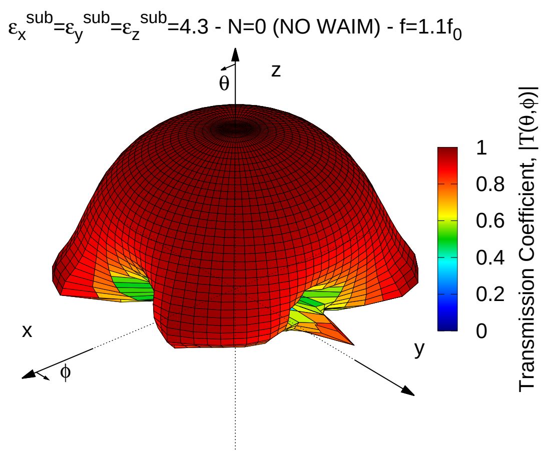

(f) $|T|^2$, No-WAIM, $f = 1.1f_0$

Figure 6: *Seed* 46, Transmission Coefficient.

Tool	*Cost Function*		*Improvement Percentage*
	Φ_0^{fine}	Φ_{SbD}^{fine}	
Truncated	551.31	592.82	7.53%

Table 2: *Seed* 46, Cost Function Improvement.

By analyzing also the results obtained from the other seeds, we can find a better solution than the one that minimizes the *Fitness Value*. In fact, the *Seed* 65 has a better overall *Cost Function* value with respect the considered *Seed* 46, even though, due to the low number of samples taken into account by the PSO that gives, it has an higher *Fitness Value*.

Tool	*Optimal Solution*				*Fitness Value*	
	$\varepsilon_x^1 = \varepsilon_y^1 = \varepsilon_z^1$	$h^1\ [\lambda]$	$\varepsilon_x^2 = \varepsilon_y^2 = \varepsilon_z^2$	$h^2\ [\lambda]$	$\Phi_{i=0}$	$\Phi_{I=200}$
Truncated	1.053	0.169	2.469	0.160	20.303	15.726

Table 3: *Seed* 65 Optimal Solution.

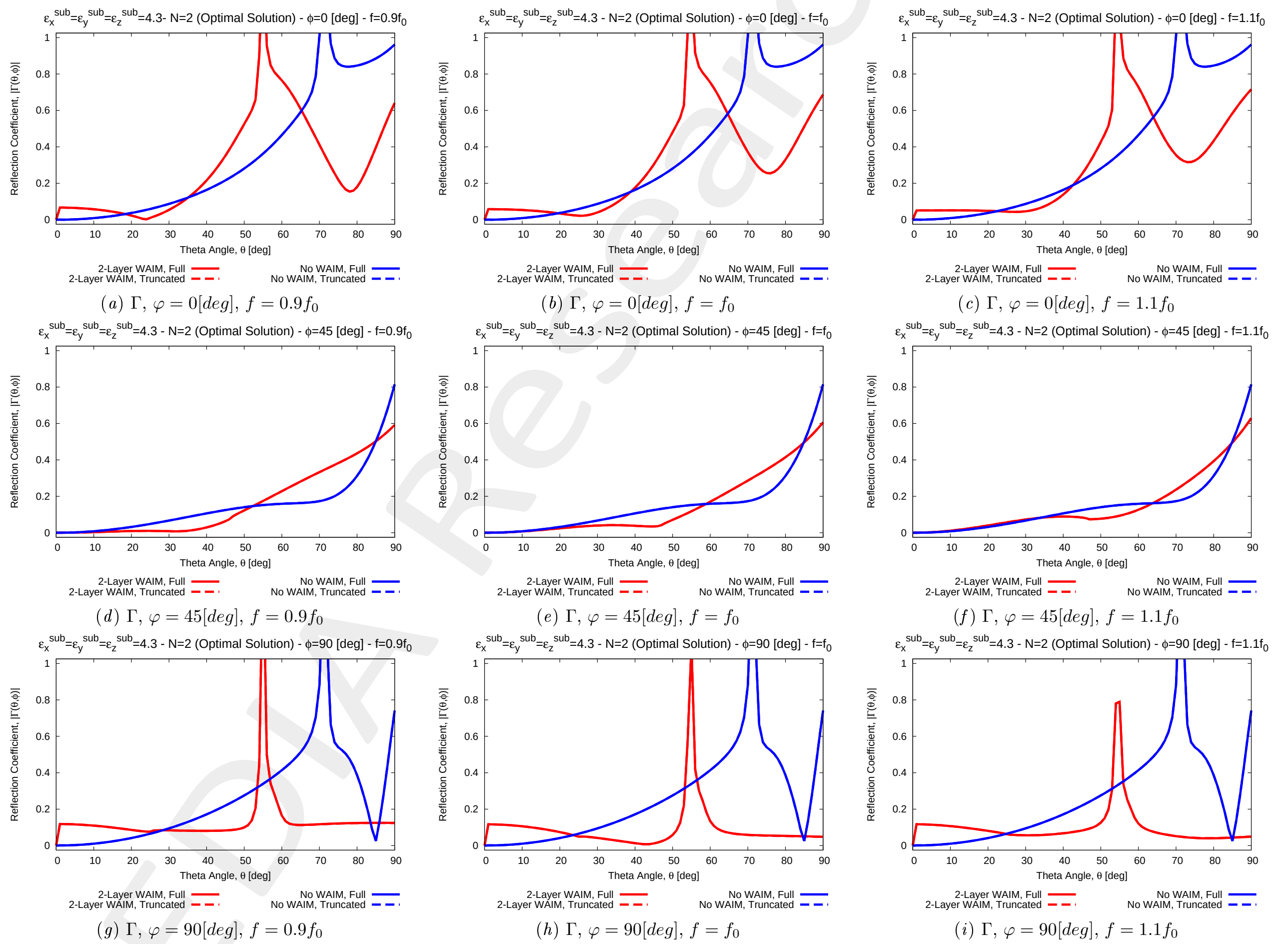

(*a*) Γ, $\varphi = 0[deg]$, $f = 0.9f_0$ (*b*) Γ, $\varphi = 0[deg]$, $f = f_0$ (*c*) Γ, $\varphi = 0[deg]$, $f = 1.1f_0$

(*d*) Γ, $\varphi = 45[deg]$, $f = 0.9f_0$ (*e*) Γ, $\varphi = 45[deg]$, $f = f_0$ (*f*) Γ, $\varphi = 45[deg]$, $f = 1.1f_0$

(*g*) Γ, $\varphi = 90[deg]$, $f = 0.9f_0$ (*h*) Γ, $\varphi = 90[deg]$, $f = f_0$ (*i*) Γ, $\varphi = 90[deg]$, $f = 1.1f_0$

Figure 7: *Seed* 65, Reflection Coefficient along φ cuts, 2 Layers WAIM.

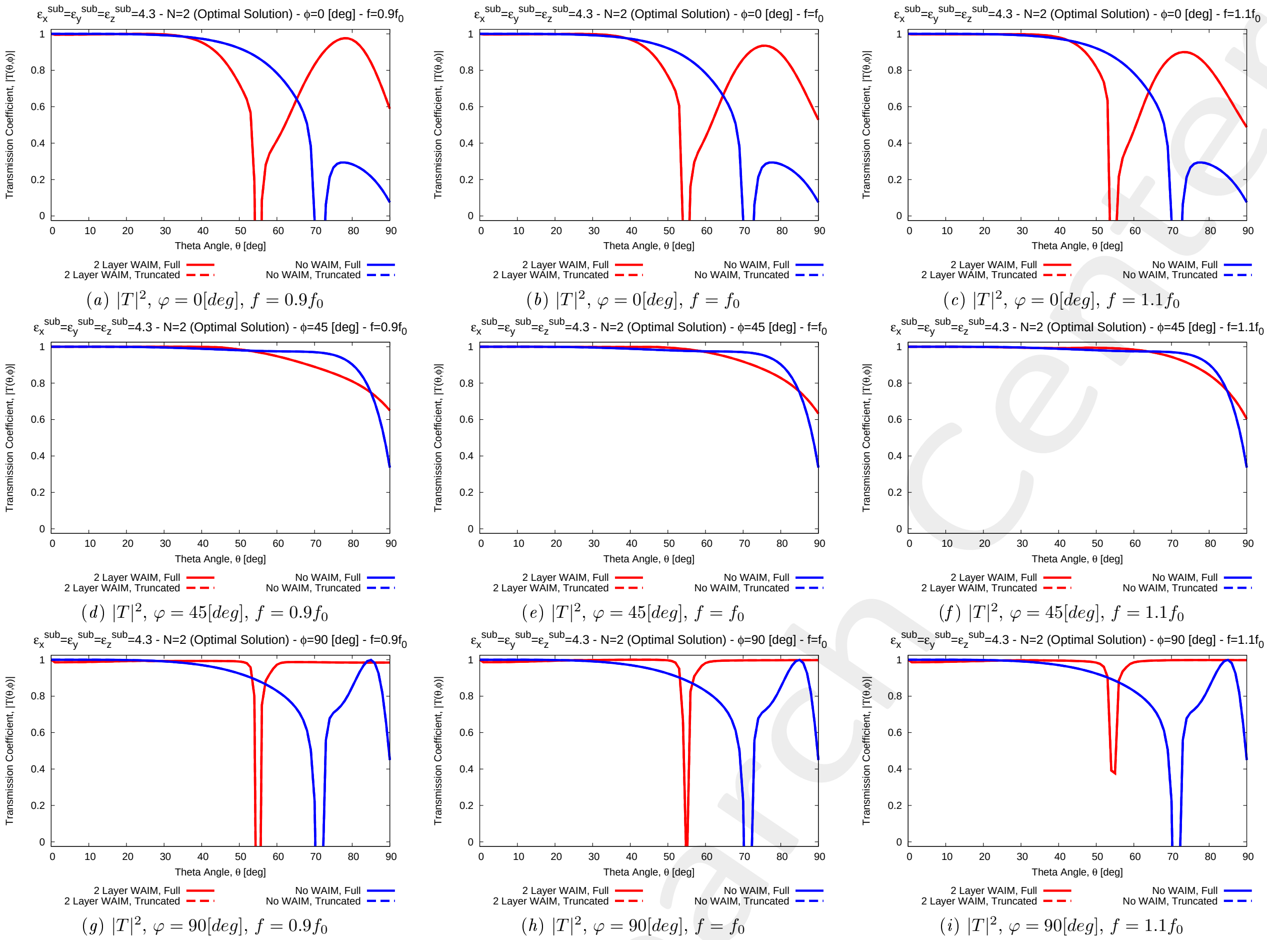

(a) $|T|^2$, $\varphi = 0[deg]$, $f = 0.9f_0$
(b) $|T|^2$, $\varphi = 0[deg]$, $f = f_0$
(c) $|T|^2$, $\varphi = 0[deg]$, $f = 1.1f_0$
(d) $|T|^2$, $\varphi = 45[deg]$, $f = 0.9f_0$
(e) $|T|^2$, $\varphi = 45[deg]$, $f = f_0$
(f) $|T|^2$, $\varphi = 45[deg]$, $f = 1.1f_0$
(g) $|T|^2$, $\varphi = 90[deg]$, $f = 0.9f_0$
(h) $|T|^2$, $\varphi = 90[deg]$, $f = f_0$
(i) $|T|^2$, $\varphi = 90[deg]$, $f = 1.1f_0$

Figure 8: *Seed* 65, Transmission Coefficient along φ cuts, 2 Layers WAIM.

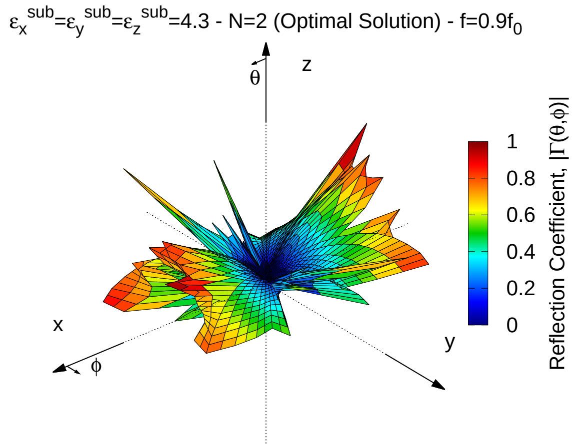

(a) Γ, 2 Layers WAIM, $f = 0.9 f_0$

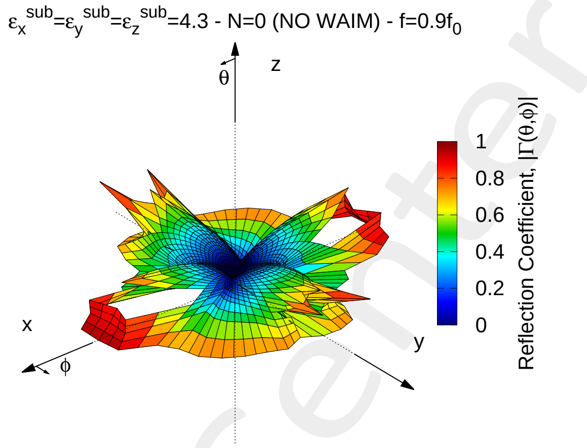

(b) Γ, No-WAIM, $f = 0.9 f_0$

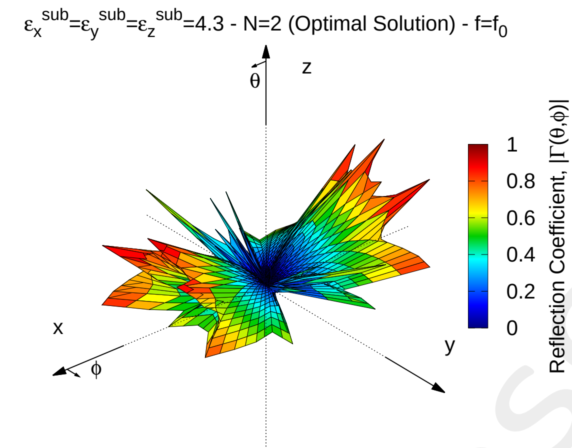

(c) Γ, 2 Layers WAIM, $f = f_0$

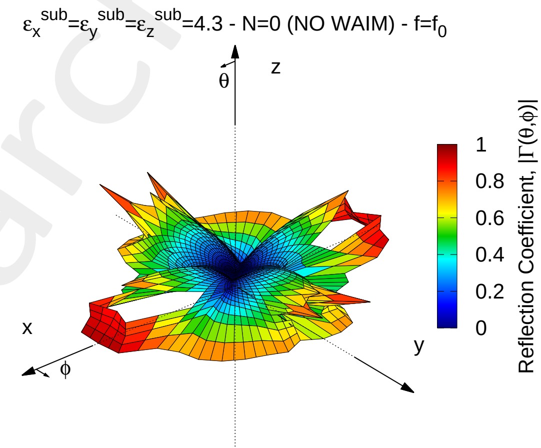

(d) Γ, No-WAIM, $f = f_0$

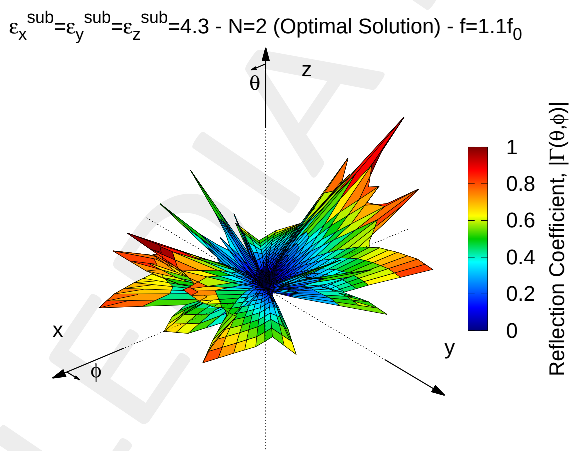

(e) Γ, 2 Layers WAIM, $f = 1.1 f_0$

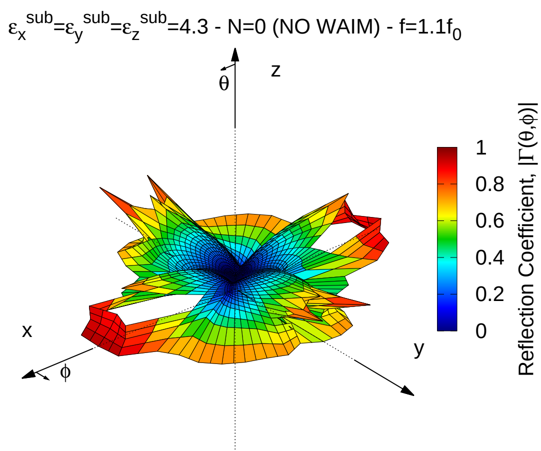

(f) Γ, No-WAIM, $f = 1.1 f_0$

Figure 9: *Seed* 65, 3D Reflection Coefficient.

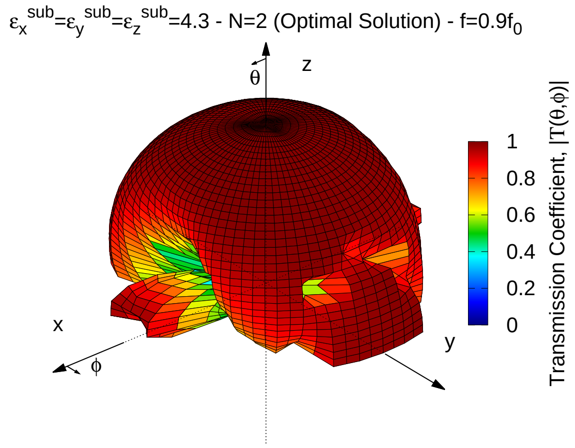

(a) $|T|^2$, 2 Layers WAIM, $f = 0.9f_0$

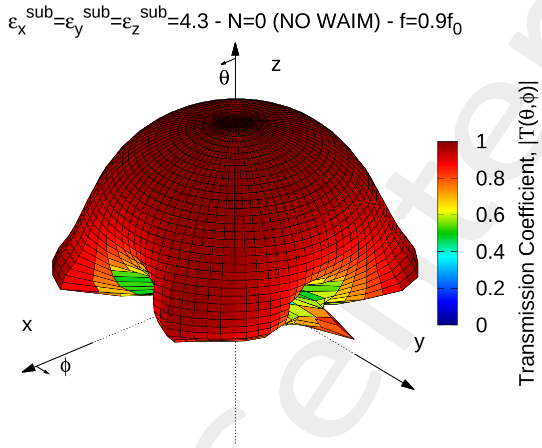

(b) $|T|^2$, No-WAIM, $f = 0.9f_0$

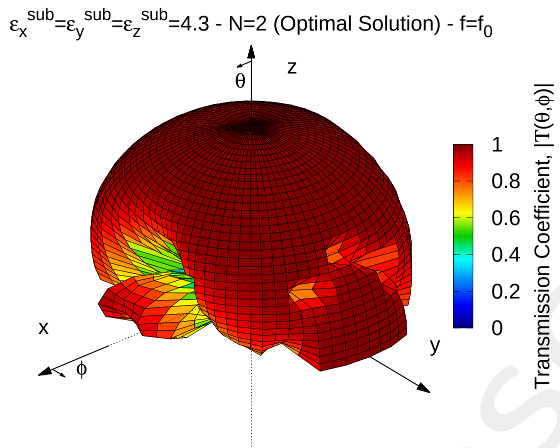

(c) $|T|^2$, 2 Layers WAIM, $f = f_0$

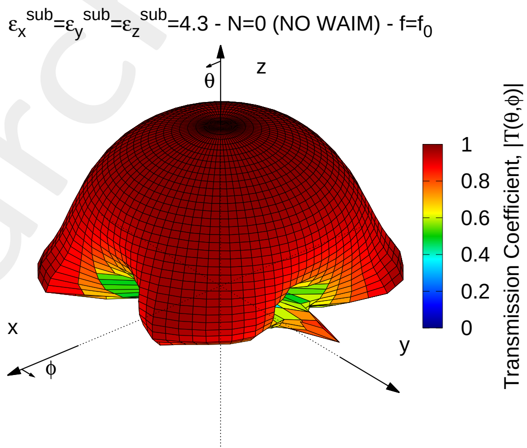

(d) $|T|^2$, No-WAIM, $f = f_0$

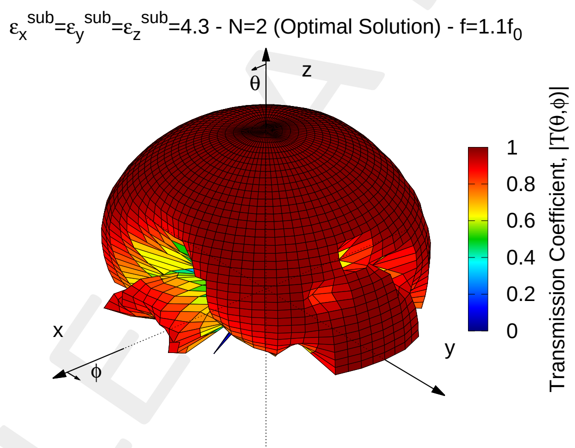

(e) $|T|^2$, 2 Layers WAIM, $f = 1.1f_0$

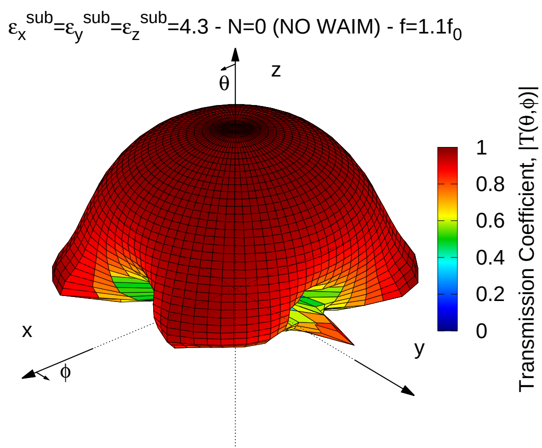

(f) $|T|^2$, No-WAIM, $f = 1.1f_0$

Figure 10: *Seed* 65, Transmission Coefficient.

Tool	*Cost Function*		*Improvement Percentage*
	Φ_0^{fine}	Φ_{SbD}^{fine}	
Truncated	551.31	454.61	-17.54%

Table 4: *Seed* 65, Cost Function Improvement.

From the results of both the analyzed solutions we can notice a non-physical behaviour of the Reflection Coefficient that, for some angles, has values $\Gamma > 1$. This causes out of bounds in the 2D plots and white regions in the 3D ones.

This phenomenon, that does not appear in other test cases in the previous sections, is be due to the fact that we are considering also the imaginary part of the substrate.

1.2 Test Case #2 - Multi frequency - 2 Isotropic WAIM Layers - $\varepsilon^1 = \varepsilon^2 = [1 : 35] + j0$ - Square Lattice - $\varepsilon^{sub} = 4.3 + j0$ Tests

We now repeat the previous test case, but this time we are considering an ideal substrate (imaginary component equal to 0).

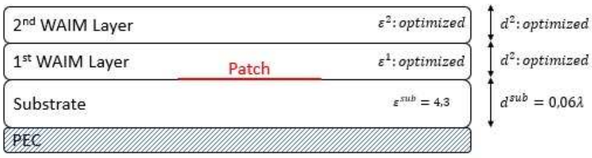

Figure 11: Test Case Schema.

Simulation Parameters:

- Frequency: $f_0 = 10[GHz]$;
- Frequency min: $f_{min} = 0.9f_0$;
- Frequency max: $f_{max} = 1.1f_0$;
- Frequency samples: $F = 3$;
- Patch dimensions: $w = 0.307$, $l = 0.2125$ $[\lambda]$;
- Probe position: $x = 0.0705$, $y = 0.1535$ $[\lambda]$;
- Substrate: $\varepsilon_x = 4.3 + j0$, $\varepsilon_y = 4.3 + j0$, $\varepsilon_z = 4.3 + j0$, $d = 0.06[\lambda]$
- Floquet coefficient = 121;
- Lattice basis: $s_1 = (0.5, 0.0)$, $s_2 = (0.0, 0.5)$ $[\lambda]$;

Analysis Parameters:

- Samples analysis (phi cuts): $\theta \in [0, 90]$ $[deg]$, $\varphi \in [0, 90]$ $[deg]$, $\theta_{samples} = 91$, $\varphi_{samples} = 3$;
- Samples analysis (3D plots): $\theta \in [-90, 90]$ $[deg]$, $\varphi \in [-90, 90]$ $[deg]$, $\theta_{samples} = 36$, $\varphi_{samples} = 21$;

PSO Synthesis Parameters:

- Number of WAIM Layers: $N = 2$;
- Unknowns: $U = 4$;
- Unknown ranges: $\varepsilon = [1 : 35] + j0$, $d = [0.033 : 0.5]$ $[\lambda]$;
- Swarm size: $P = 12$;

- Max iteration number: $I = 200$;
- Inertial weight= 0.4;
- Alpha= 0.4;
- Beta= 0.4;
- C1= 2.0;
- C2= 2.0;
- Random seeds= 6, 12, 26, 33, 46, 51, 65, 77, 98;
- No-WAIM case implemented by the first particle at the 1^{st} iteration;
- Samples synthesis (phi cuts): $\theta \in [0, 90]$ $[deg]$, $\varphi \in [0, 90]$ $[deg]$, $\theta_{samples} = 7$, $\varphi_{samples} = 3$;

Optimization Results

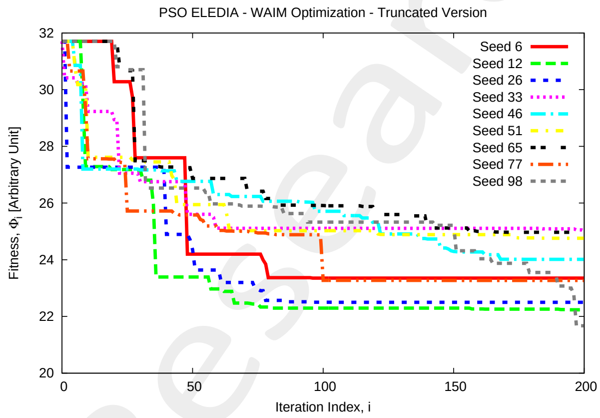

Figure 12: Fitness Dynamics.

$$Best\,result:\ Seed\,98$$

$$Simulation\,time\,(Truncated):\ 1162m\,38s$$

$Tool$	$Optimal\,Solution$				$Fitness\,Value$	
	$\varepsilon_x^1 = \varepsilon_y^1 = \varepsilon_z^1$	$h^1\,[\lambda]$	$\varepsilon_x^2 = \varepsilon_y^2 = \varepsilon_z^2$	$h^2\,[\lambda]$	$\Phi_{i=0}$	$\Phi_{I=200}$
$Truncated$	5.894	0.033	32.933	0.033	31.703	21.672

Table 5: $Seed\,98$ Optimal Solution.

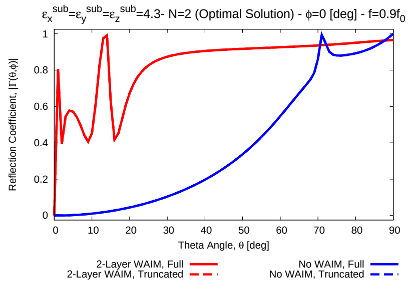

$(a)\ \Gamma,\ \varphi = 0[deg],\ f = 0.9f_0$

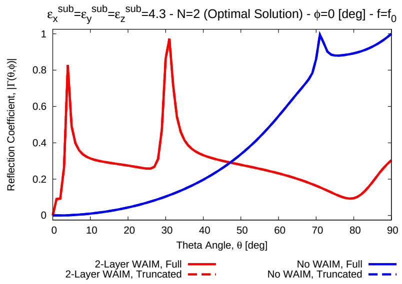

$(b)\ \Gamma,\ \varphi = 0[deg],\ f = f_0$

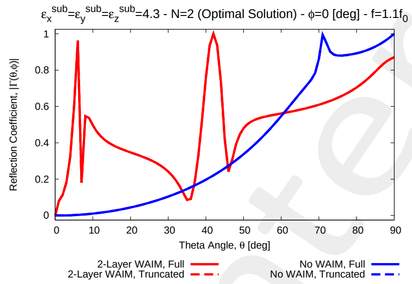

$(c)\ \Gamma,\ \varphi = 0[deg],\ f = 1.1f_0$

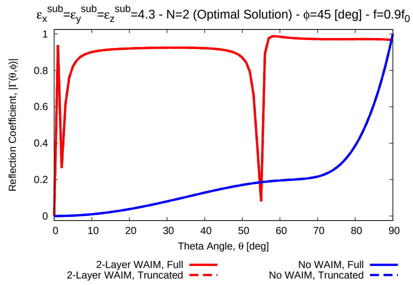

$(d)\ \Gamma,\ \varphi = 45[deg],\ f = 0.9f_0$

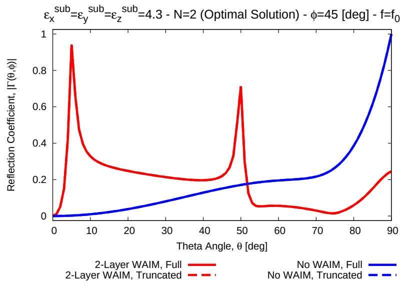

$(e)\ \Gamma,\ \varphi = 45[deg],\ f = f_0$

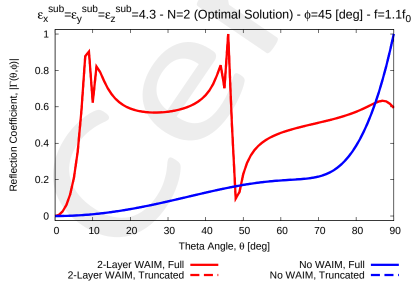

$(f)\ \Gamma,\ \varphi = 45[deg],\ f = 1.1f_0$

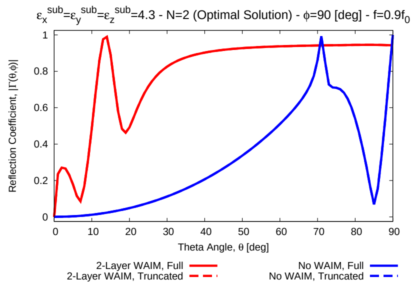

$(g)\ \Gamma,\ \varphi = 90[deg],\ f = 0.9f_0$

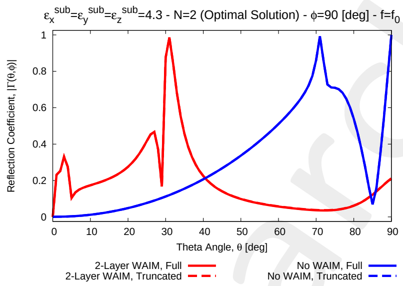

$(h)\ \Gamma,\ \varphi = 90[deg],\ f = f_0$

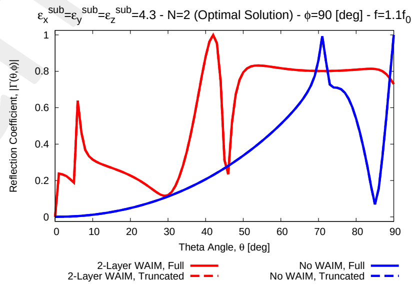

$(i)\ \Gamma,\ \varphi = 90[deg],\ f = 1.1f_0$

Figure 13: *Seed* 98, Reflection Coefficient along φ cuts, 2 Layers WAIM.

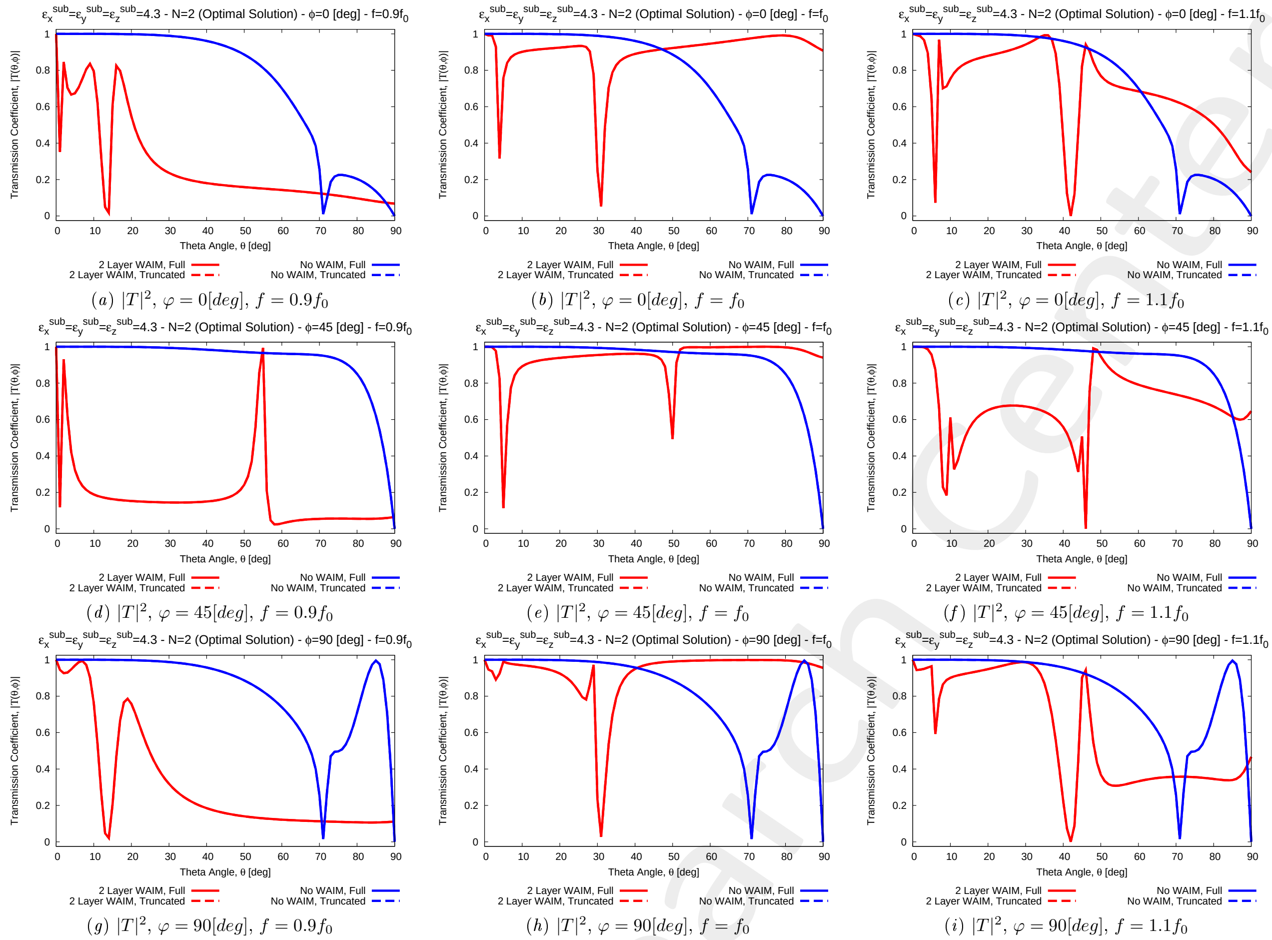

Figure 14: *Seed* 98, Transmission Coefficient along φ cuts, 2 Layers WAIM.

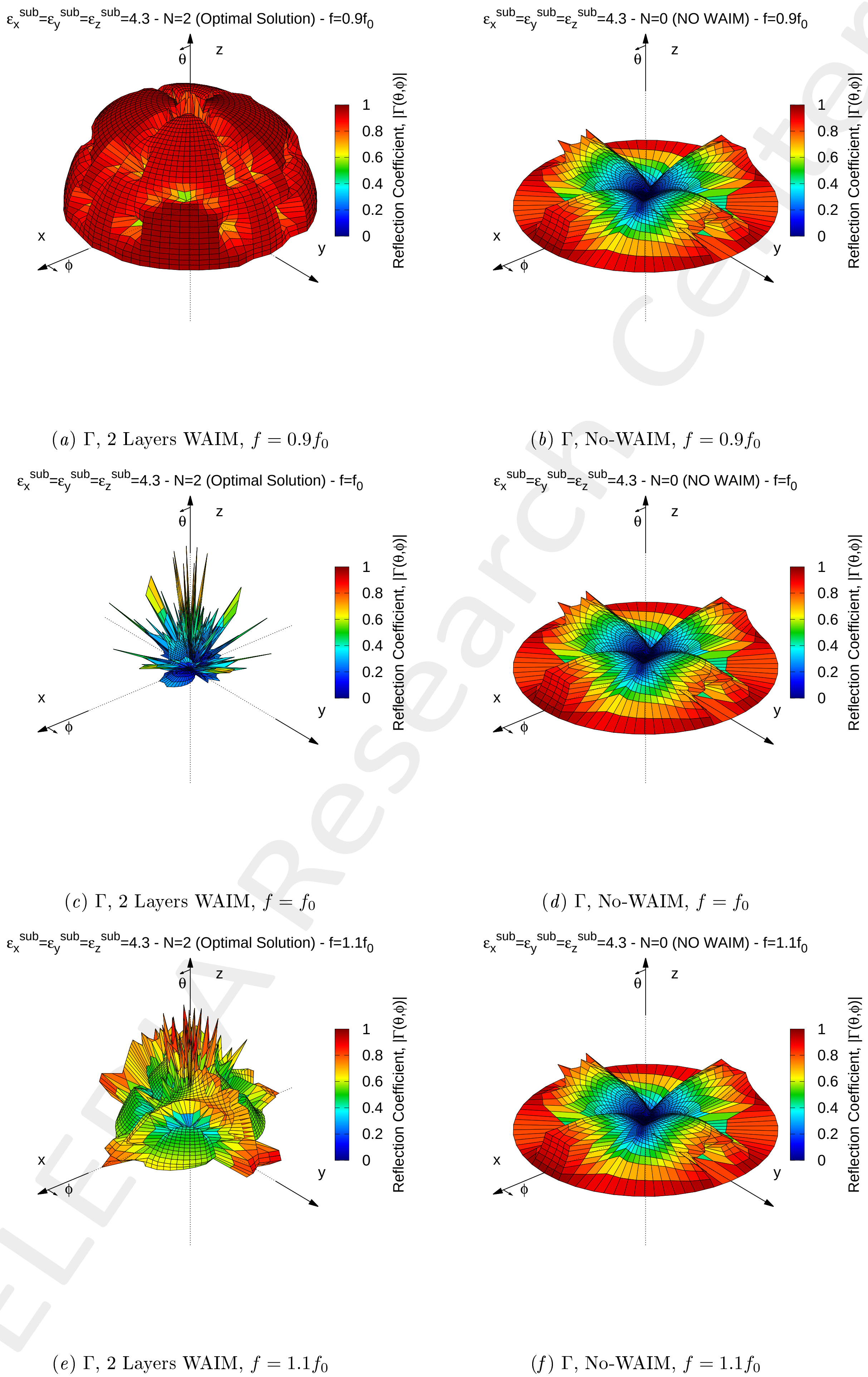

(a) Γ, 2 Layers WAIM, $f = 0.9f_0$ (b) Γ, No-WAIM, $f = 0.9f_0$

(c) Γ, 2 Layers WAIM, $f = f_0$ (d) Γ, No-WAIM, $f = f_0$

(e) Γ, 2 Layers WAIM, $f = 1.1f_0$ (f) Γ, No-WAIM, $f = 1.1f_0$

Figure 15: *Seed* 98, 3D Reflection Coefficient.

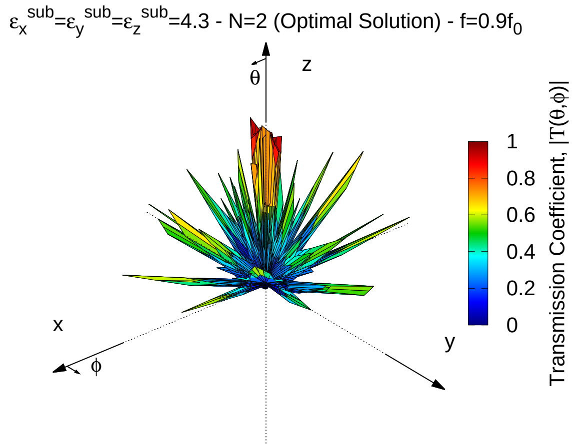

(a) $|T|^2$, 2 Layers WAIM, $f = 0.9f_0$

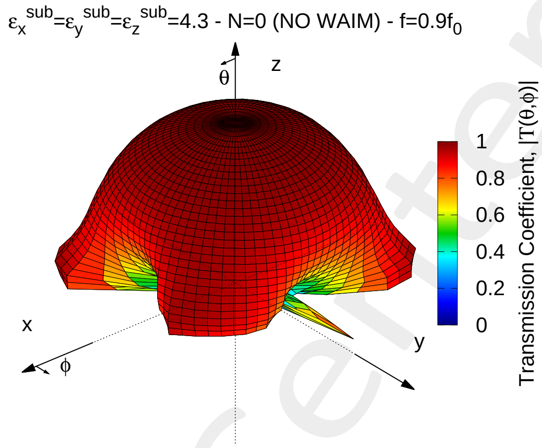

(b) $|T|^2$, No-WAIM, $f = 0.9f_0$

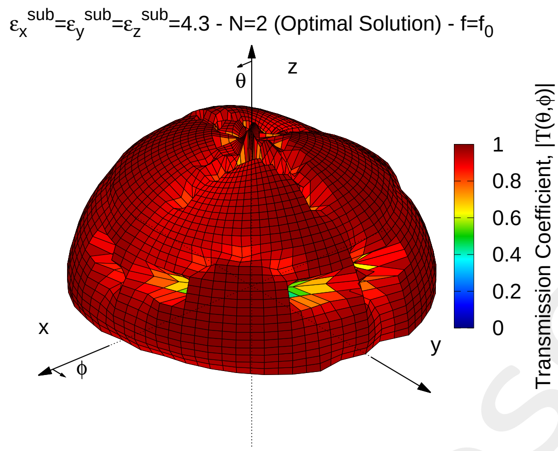

(c) $|T|^2$, 2 Layers WAIM, $f = f_0$

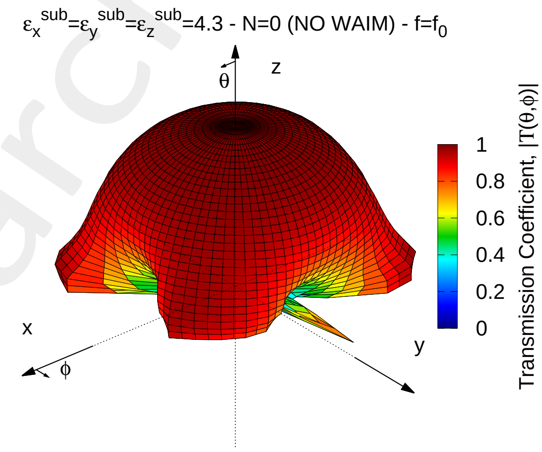

(d) $|T|^2$, No-WAIM, $f = f_0$

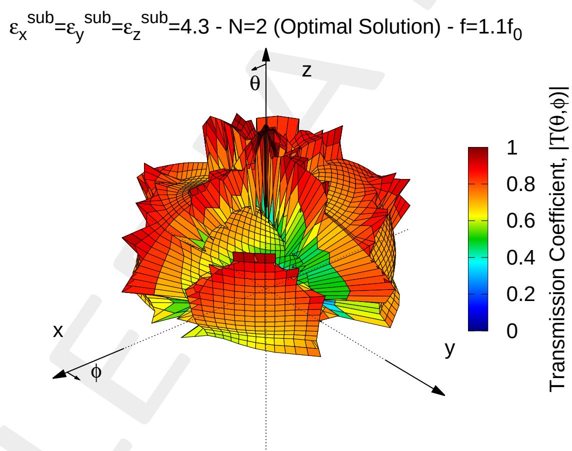

(e) $|T|^2$, 2 Layers WAIM, $f = 1.1f_0$

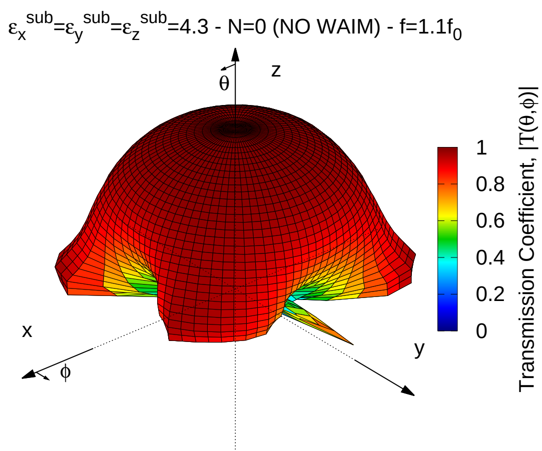

(f) $|T|^2$, No-WAIM, $f = 1.1f_0$

Figure 16: *Seed* 98, Transmission Coefficient.

$Tool$	$Cost\ Function$		$Improvement\ Percentage$
	Φ_0^{fine}	Φ_{SbD}^{fine}	
$Truncated$	663.75	1202.34	81.14%

Table 6: *Seed* 98, Cost Function Improvement.

Once again, by analyzing also the results obtained from the other seeds, we can find a better solution in *Seed* 65.

$Tool$	$Optimal\ Solution$				$Fitness\ Value$	
	$\varepsilon_x^1 = \varepsilon_y^1 = \varepsilon_z^1$	$h^1\ [\lambda]$	$\varepsilon_x^2 = \varepsilon_y^2 = \varepsilon_z^2$	$h^2\ [\lambda]$	$\Phi_{i=0}$	$\Phi_{I=200}$
$Truncated$	1.198	0.033	3.102	0.034	31.703	24.971

Table 7: *Seed* 65 Optimal Solution.

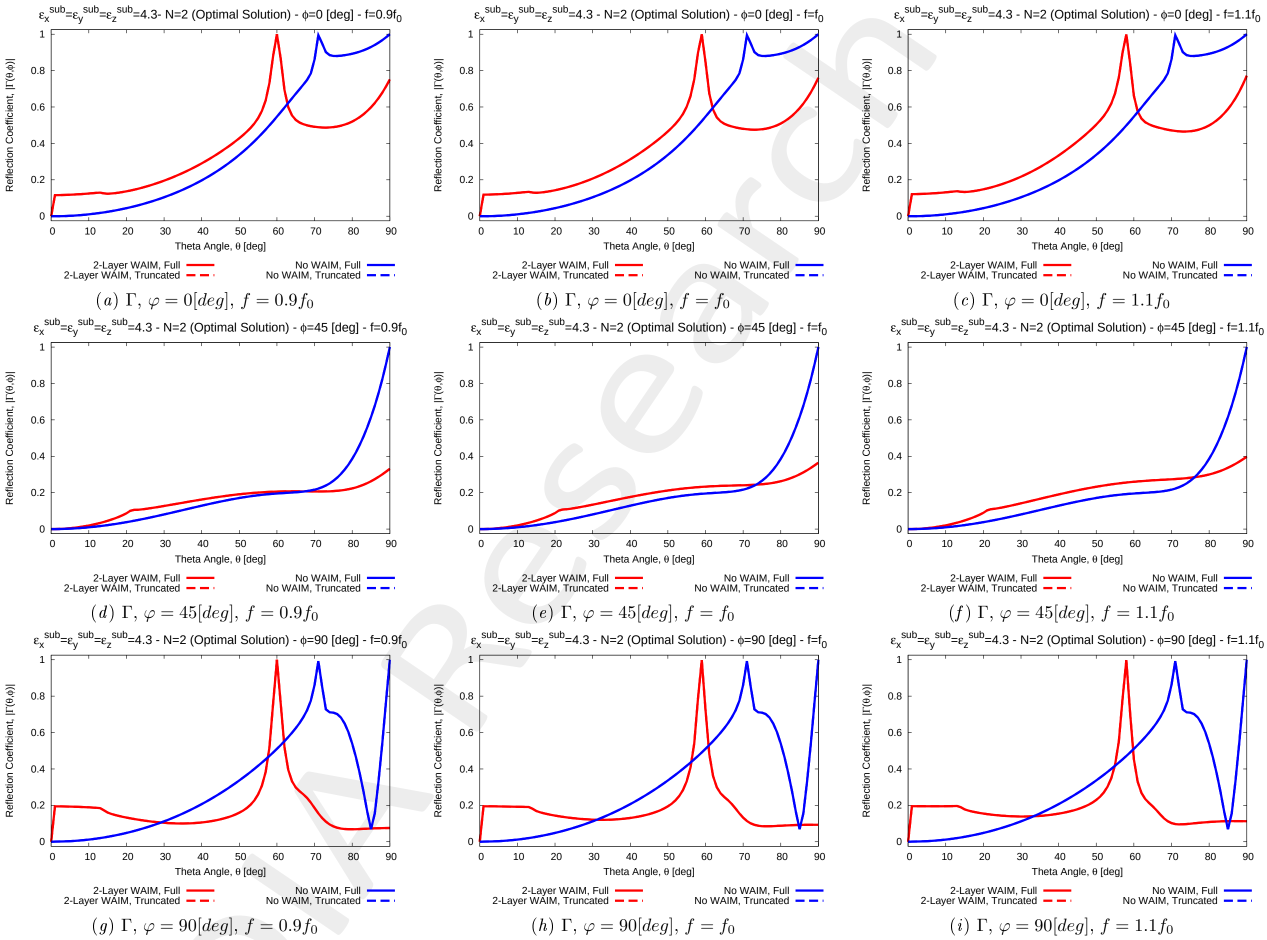

(a) Γ, $\varphi = 0[deg]$, $f = 0.9f_0$ (b) Γ, $\varphi = 0[deg]$, $f = f_0$ (c) Γ, $\varphi = 0[deg]$, $f = 1.1f_0$

(d) Γ, $\varphi = 45[deg]$, $f = 0.9f_0$ (e) Γ, $\varphi = 45[deg]$, $f = f_0$ (f) Γ, $\varphi = 45[deg]$, $f = 1.1f_0$

(g) Γ, $\varphi = 90[deg]$, $f = 0.9f_0$ (h) Γ, $\varphi = 90[deg]$, $f = f_0$ (i) Γ, $\varphi = 90[deg]$, $f = 1.1f_0$

Figure 17: *Seed* 65, Reflection Coefficient along φ cuts, 2 Layers WAIM.

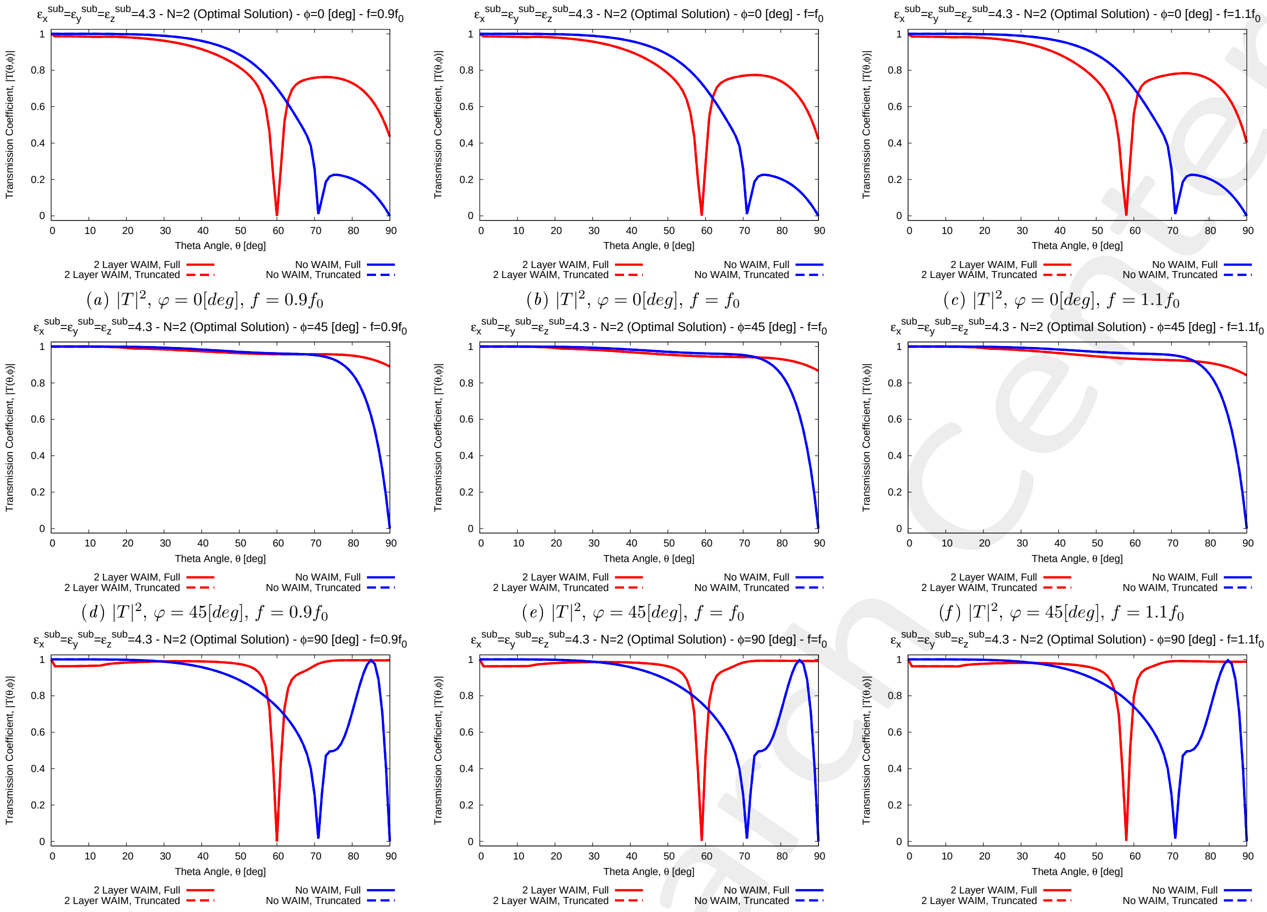

(a) $|T|^2$, $\varphi = 0[deg]$, $f = 0.9f_0$
(b) $|T|^2$, $\varphi = 0[deg]$, $f = f_0$
(c) $|T|^2$, $\varphi = 0[deg]$, $f = 1.1f_0$
(d) $|T|^2$, $\varphi = 45[deg]$, $f = 0.9f_0$
(e) $|T|^2$, $\varphi = 45[deg]$, $f = f_0$
(f) $|T|^2$, $\varphi = 45[deg]$, $f = 1.1f_0$
(g) $|T|^2$, $\varphi = 90[deg]$, $f = 0.9f_0$
(h) $|T|^2$, $\varphi = 90[deg]$, $f = f_0$
(i) $|T|^2$, $\varphi = 90[deg]$, $f = 1.1f_0$

Figure 18: *Seed* 65, Transmission Coefficient along φ cuts, 2 Layers WAIM.

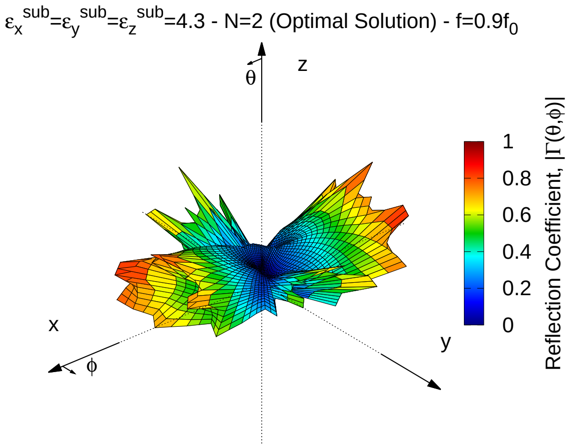

(a) Γ, 2 Layers WAIM, $f = 0.9f_0$

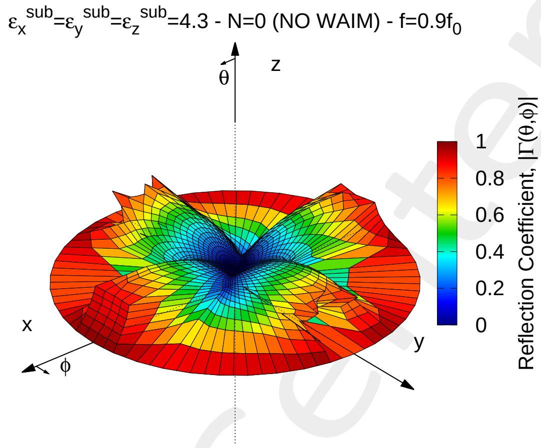

(b) Γ, No-WAIM, $f = 0.9f_0$

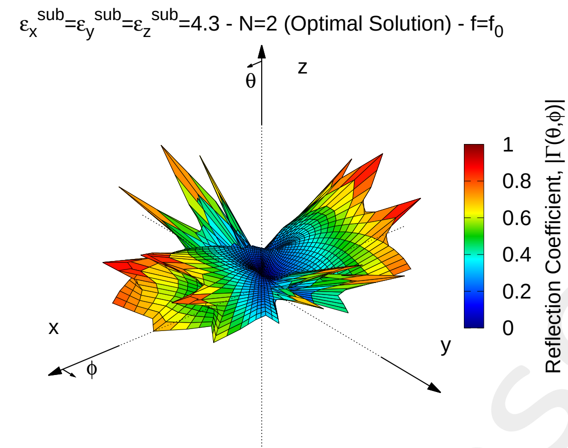

(c) Γ, 2 Layers WAIM, $f = f_0$

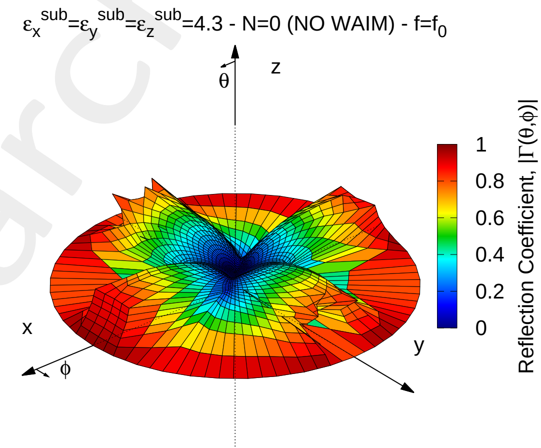

(d) Γ, No-WAIM, $f = f_0$

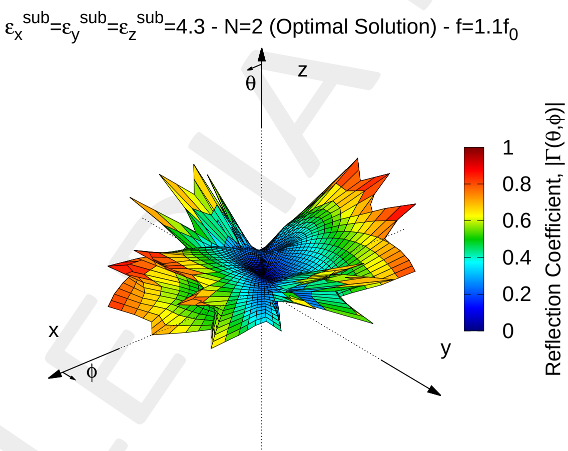

(e) Γ, 2 Layers WAIM, $f = 1.1f_0$

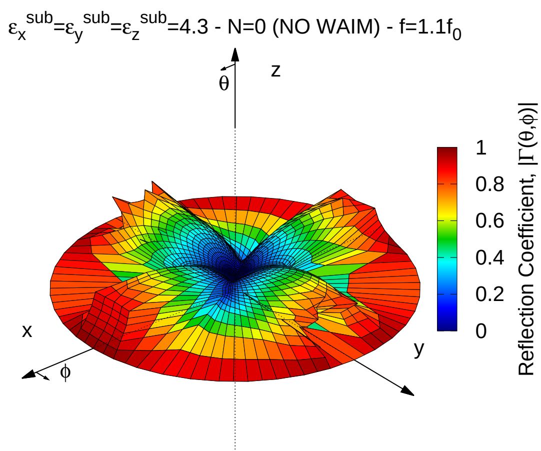

(f) Γ, No-WAIM, $f = 1.1f_0$

Figure 19: *Seed* 65, 3D Reflection Coefficient.

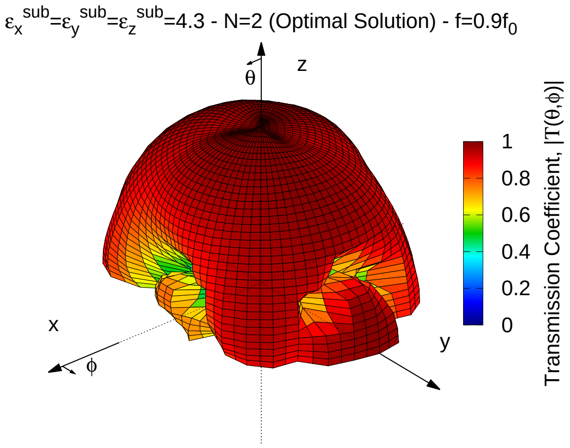

(*a*) $|T|^2$, 2 Layers WAIM, $f = 0.9f_0$

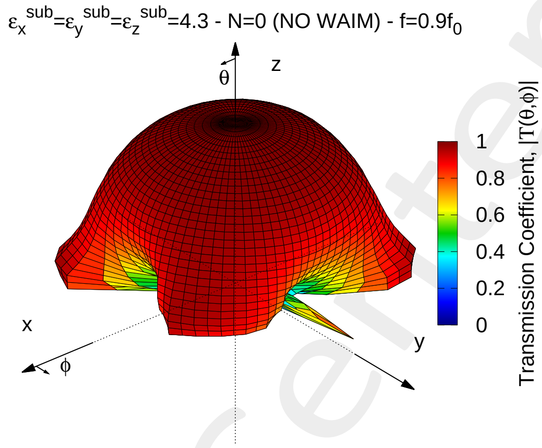

(*b*) $|T|^2$, No-WAIM, $f = 0.9f_0$

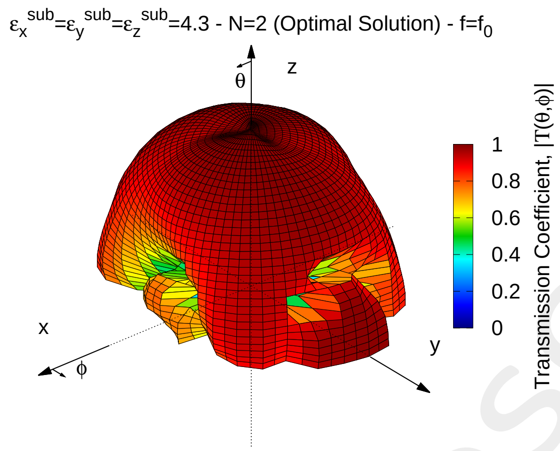

(*c*) $|T|^2$, 2 Layers WAIM, $f = f_0$

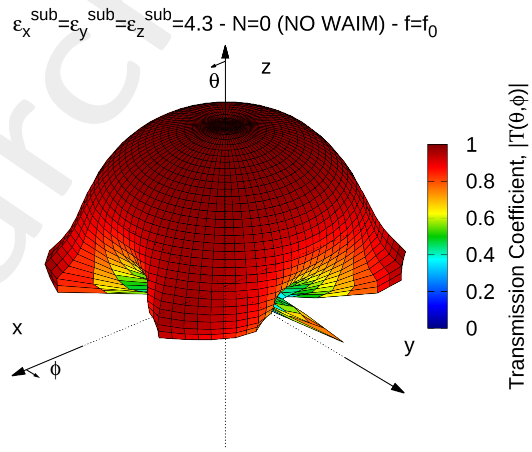

(*d*) $|T|^2$, No-WAIM, $f = f_0$

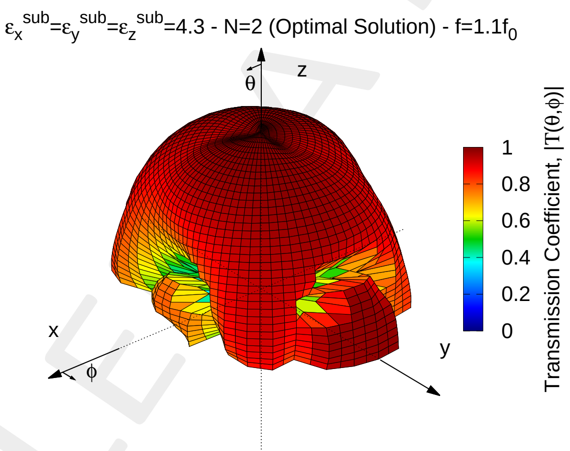

(*e*) $|T|^2$, 2 Layers WAIM, $f = 1.1f_0$

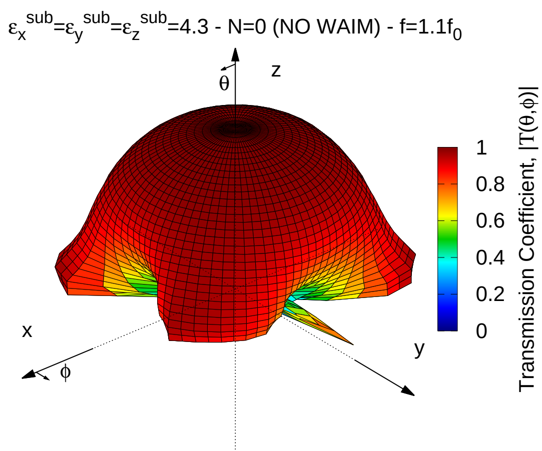

(*f*) $|T|^2$, No-WAIM, $f = 1.1f_0$

Figure 20: *Seed* 65, Transmission Coefficient.

$Tool$	$Cost\ Function$		$Improvement\ Percentage$
	Φ_0^{fine}	Φ_{SbD}^{fine}	
$Truncated$	663.75	662.62	-0.17%

Table 8: $Seed$ 65, Cost Function Improvement.

By considering an ideal substrate we solved the problem of non-physical behaviour of the Reflection Coefficient, that now has always values $\Gamma < 1$. However, both the covered and the non-covered *Cost Function* values ($\Phi_0^{fine} = 663.75$ and $\Phi_{SbD}^{fine} = 662.62$) are quite different and in general higher then the results obtained in 1.1 for a real substrate ($\Phi_0^{fine} = 551.31$ and $\Phi_{SbD}^{fine} = 454.61$).

More information on the topics of this document can be found in the following list of references.

References

[1] P. Rocca, M. Benedetti, M. Donelli, D. Franceschini, and A. Massa, "Evolutionary optimization as applied to inverse problems," Inverse Problems - 25 th Year Special Issue of Inverse Problems, Invited Topical Review, vol. 25, pp. 1-41, Dec. 2009.

[2] P. Rocca, G. Oliveri, and A. Massa, "Differential Evolution as applied to electromagnetics," IEEE Antennas Propag. Mag., vol. 53, no. 1, pp. 38-49, Feb. 2011.

[3] P. Rocca, N. Anselmi, A. Polo, and A. Massa, "An irregular two-sizes square tiling method for the design of isophoric phased arrays," IEEE Trans. Antennas Propag., vol. 68, no. 6, pp. 4437-4449, Jun. 2020.

[4] P. Rocca, N. Anselmi, A. Polo, and A. Massa, "Modular design of hexagonal phased arrays through diamond tiles," IEEE Trans. Antennas Propag., vol.68, no. 5, pp. 3598-3612, May 2020.

[5] N. Anselmi, L. Poli, P. Rocca, and A. Massa, "Design of simplified array layouts for preliminary experimental testing and validation of large AESAs," IEEE Trans. Antennas Propag., vol. 66, no. 12, pp. 6906-6920, Dec. 2018.

[6] N. Anselmi, P. Rocca, M. Salucci, and A. Massa, "Contiguous phase-clustering in multibeam-on-receive scanning arrays" IEEE Trans. Antennas Propag., vol. 66, no. 11, pp. 5879-5891, Nov. 2018.

[7] G. Oliveri, G. Gottardi, F. Robol, A. Polo, L. Poli, M. Salucci, M. Chuan, C. Massagrande, P. Vinetti, M. Mattivi, R. Lombardi, and A. Massa, "Co-design of unconventional array architectures and antenna elements for 5G base station," IEEE Trans. Antennas Propag., vol. 65, no. 12, pp. 6752-6767, Dec. 2017.

[8] N. Anselmi, P. Rocca, M. Salucci, and A. Massa, "Irregular phased array tiling by means of analytic schemata-driven optimization," IEEE Trans. Antennas Propag., vol. 65, no. 9, pp. 4495-4510, September 2017.

[9] N. Anselmi, P. Rocca, M. Salucci, and A. Massa, "Optimization of excitation tolerances for robust beamforming in linear arrays" IET Microwaves, Antennas & Propagation, vol. 10, no. 2, pp. 208-214, 2016.

[10] P. Rocca, R. J. Mailloux, and G. Toso, "GA-Based optimization of irregular sub-array layouts for wideband phased arrays desig," IEEE Antennas and Wireless Propag. Lett., vol. 14, pp. 131-134, 2015.

[11] P. Rocca, M. Donelli, G. Oliveri, F. Viani, and A. Massa, "Reconfigurable sum-difference pattern by means of parasitic elements for forward-looking monopulse radar," IET Radar, Sonar & Navigation, vol 7, no. 7, pp. 747-754, 2013.

[12] P. Rocca, L. Manica, and A. Massa, "Ant colony based hybrid approach for optimal compromise sum-difference patterns synthesis," Microwave Opt. Technol. Lett., vol. 52, no. 1, pp. 128-132, Jan. 2010.

[13] P. Rocca, L. Manica, and A. Massa, "An improved excitation matching method based on an ant colony optimization for suboptimal-free clustering in sum-difference compromise synthesis," IEEE Trans. Antennas Propag., vol. 57, no. 8, pp. 2297-2306, Aug. 2009.

[14] P. Rocca, L. Manica, and A. Massa, "Hybrid approach for sub-arrayed monopulse antenna synthesis," Electronics Letters, vol. 44, no. 2, pp. 75-76, Jan. 2008.

[15] P. Rocca, L. Manica, F. Stringari, and A. Massa, "Ant colony optimization for tree-searching based synthesis of monopulse array antenna," Electronics Letters, vol. 44, no. 13, pp. 783-785, Jun. 19, 2008.

[16] G. Oliveri, A. Gelmini, A. Polo, N. Anselmi, and A. Massa, "System-by-design multi-scale synthesis of task-oriented reflectarrays," IEEE Trans. Antennas Propag., vol. 68, no. 4, pp. 2867-2882, Apr. 2020.

[17] M. Salucci, F. Robol, N. Anselmi, M. A. Hannan, P. Rocca, G. Oliveri, M. Donelli, and A. Massa, "S-Band spline-shaped aperture-stacked patch antenna for air traffic control applications," IEEE Tran. Antennas Propag., vol. 66, no. 8, pp. 4292-4297, Aug. 2018.

[18] M. Salucci, L. Poli, A. F. Morabito, and P. Rocca, "Adaptive nulling through subarray switching in planar antenna arrays," Journal of Electromagnetic Waves and Applications, vol. 30, no. 3, pp. 404-414, February 2016

[19] T. Moriyama, L. Poli, and P. Rocca, "Adaptive nulling in thinned planar arrays through genetic algorithms" IEICE Electronics Express, vol. 11, no. 21, pp. 1-9, Sep. 2014.

[20] L. Poli, P. Rocca, M. Salucci, and A. Massa, "Reconfigurable thinning for the adaptive control of linear arrays," IEEE Trans. Antennas Propag., vol. 61, no. 10, pp. 5068-5077, Oct. 2013.

[21] P. Rocca, L. Poli, G. Oliveri, and A. Massa, "Adaptive nulling in time-varying scenarios through time-modulated linear arrays," IEEE Antennas Wireless Propag. Lett., vol. 11, pp. 101-104, 2012.

[22] M. Benedetti, G. Oliveri, P. Rocca, and A. Massa, "A fully-adaptive smart antenna prototype: ideal model and experimental validation in complex interference scenarios," Progress in Electromagnetic Research, PIER 96, pp. 173-191, 2009.

[23] M. Benedetti, R. Azaro, and A. Massa, "Memory enhanced PSO-based optimization approach for smart antennas control in complex interference scenarios," IEEE Trans. Antennas Propag., vol. 56, no. 7, pp. 1939-1947, Jul. 2008.

[24] M. Benedetti, R. Azaro, and A. Massa, "Experimental validation of a fully-adaptive smart antenna prototype," Electronics Letters, vol. 44, no. 11, pp. 661-662, May 2008.

[25] R. Azaro, L. Ioriatti, M. Martinelli, M. Benedetti, and A. Massa, "An experimental realization of a fully-adaptive smart antenna," Microwave Opt. Technol. Lett., vol. 50, no. 6, pp. 1715-1716, Jun. 2008.

[26] M. Benedetti, R. Azaro, D. Franceschini, and A. Massa, "PSO-based real-time control of planar uniform circular arrays," IEEE Antennas Wireless Propag. Lett., vol. 5, pp. 545-548, 2006.

[27] G. Oliveri, P. Rocca, M. Salucci, and A. Massa, "Holographic smart EM skins for advanced beam power shaping in next generation wireless environments," IEEE J. Multiscale Multiphysics Comput. Tech., vol. 6, pp. 171-182, Oct. 2021.

[28] M. Salucci, L. Tenuti, G. Gottardi, A. Hannan, and A. Massa, "System-by-design method for efficient linear array miniaturisation through low-complexity isotropic lenses" Electronic Letters, vol. 55, no. 8, pp. 433-434, May 2019.

[29] M. Salucci, N. Anselmi, S. Goudos, and A. Massa, "Fast design of multiband fractal antennas through a system-by-design approach for NB-IoT applications" EURASIP J. Wirel. Commun. Netw., vol. 2019, no. 1, pp. 68-83, Mar. 2019.

[30] M. Salucci, G. Oliveri, N. Anselmi, and A. Massa, "Material-by-design synthesis of conformal miniaturized linear phased arrays," IEEE Access, vol. 6, pp. 26367-26382, 2018.

[31] M. Salucci, G. Oliveri, N. Anselmi, G. Gottardi, and A. Massa, "Performance enhancement of linear active electronically-scanned arrays by means of MbD-synthesized metalenses," Journal of Electromagnetic Waves and Applications, vol. 32, no. 8, pp. 927-955, 2018.

[32] G. Oliveri, M. Salucci, N. Anselmi and A. Massa, "Multiscale System-by-Design synthesis of printed WAIMs for waveguide array enhancement," IEEE J. Multiscale Multiphysics Computat. Techn., vol. 2, pp. 84-96, 2017.

[33] A. Massa and G. Oliveri, "Metamaterial-by-Design: Theory, methods, and applications to communications and sensing - Editorial," EPJ Applied Metamaterials, vol. 3, no. E1, pp. 1-3, 2016.

[34] G. Oliveri, F. Viani, N. Anselmi, and A. Massa, "Synthesis of multi-layer WAIM coatings for planar phased arrays within the system-by-design framework," IEEE Trans. Antennas Propag., vol. 63, no. 6, pp. 2482-2496, June 2015.

[35] G. Oliveri, L. Tenuti, E. Bekele, M. Carlin, and A. Massa, "An SbD-QCTO approach to the synthesis of isotropic metamaterial lenses" IEEE Antennas Wireless Propag. Lett., vol. 13, pp. 1783-1786, 2014.

[36] A. Massa, G. Oliveri, P. Rocca, and F. Viani, "System-by-Design: a new paradigm for handling design complexity," 8th European Conference on Antennas Propag. (EuCAP 2014), The Hague, The Netherlands, pp. 1180-1183, Apr. 6-11, 2014.

[37] P. Rocca, G. Oliveri, R. J. Mailloux, and A. Massa, "Unconventional phased array architectures and design Methodologies - A review," Proceedings of the IEEE, vol. 104, no. 3, pp. 544-560, March 2016.

[38] A. Massa, A. Benoni, P. Da RÃ^{1}, S. K. Goudos, B. Li, G. Oliveri, A. Polo, P. Rocca, and M. Salucci, "Designing smart electromagnetic environments for next-generation wireless communications," Telecom, Invited Paper, vol. 2, pp. 213â221, 2021.

[39] G. Oliveri, D. H. Werner, and A. Massa, "Reconfigurable electromagnetics through metamaterials - A review" Proc. IEEE, vol. 103, no. 7, pp. 1034-1056, Jul. 2015.

[40] I. Martinez, A. H. Panaretos, D. H. Werner, G. Oliveri, and A. Massa, "Ultra-thin reconfigurable electromagnetic metasurface absorbers," EuCAP 2013, Gothenburg, Sweden, Apr. 8-12, 2013.